

Mask-informed Deep Contrastive Incomplete Multi-view Clustering

Zhenglai Li^{*1} Yuqi Shi^{*2} Xiao He³ Chang Tang³

Abstract

Multi-view clustering (MvC) utilizes information from multiple views to uncover the underlying structures of data. Despite significant advancements in MvC, mitigating the impact of missing samples in specific views on the integration of knowledge from different views remains a critical challenge. This paper proposes a novel Mask-informed Deep Contrastive Incomplete Multi-view Clustering (Mask-IMvC) method, which elegantly identifies a view-common representation for clustering. Specifically, we introduce a mask-informed fusion network that aggregates incomplete multi-view information while considering the observation status of samples across various views as a mask, thereby reducing the adverse effects of missing values. Additionally, we design a prior knowledge-assisted contrastive learning loss that boosts the representation capability of the aggregated view-common representation by injecting neighborhood information of samples from different views. Finally, extensive experiments are conducted to demonstrate the superiority of the proposed Mask-IMvC method over state-of-the-art approaches across multiple MvC datasets, both in complete and incomplete scenarios.

1. Introduction

Multi-view data commonly appears in many real-world applications with the rapid development of diverse feature descriptors and data collectors (Zhou et al., 2024; Wang, 2021; Wang et al., 2023b). For instance, the visual, text, and audio information are extracted and exploited in various video understanding tasks (Li et al., 2024b; Schiappa et al., 2023). To handle this type of data, multi-view learning methods are proposed to integrate the information from various views to achieve compatible performance than the

^{*}Equal contribution ¹Faculty of Data Science, City University of Macau, Macau, China ²Faculty of Science and Technology, University of Macau, Macau, China ³School of Computer Science, China University of Geosciences, Wuhan, China. Correspondence to: Chang Tang <tangchang@cug.edu.cn>.

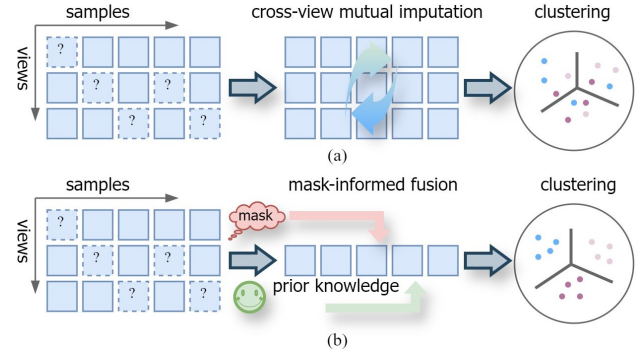


Figure 1. Comparison of two different IMvC paradigms. (a) The imputation-based IMvC. (b) Our proposed mask-informed deep contrastive IMvC.

approaches individually trained on a single view (Li et al., 2024b). Multi-view clustering (MvC), one of the kinds of multi-view learning methods, groups the data points into their respective clusters by exploring the comprehensive information among various views without labels, and has received much attention in recent years (Zhou et al., 2024; Zou et al., 2023; 2024).

In many real-world applications, the samples in particular views may be absent due to hardware faults or interference signals during information collection, resulting in incomplete multi-view data (Wen et al., 2024). The incomplete multi-view clustering (IMvC) methods are introduced to address this type of data and have witnessed great progress recently (Wen et al., 2024; Lin et al., 2021). Previous IMvC approaches mainly perform cross-view imputation to recover the absent information among different views based on cross-view semantic consistency as illustrated in Fig. 1 (a). For example, Li et al. (Li et al., 2023) introduced a prototype-based imputation manner that utilizes a dual-attention equipped with a contrastive loss to seek prototypes of each view for recovering the missing views. Pu et al. (Pu et al., 2024) designed an adaptive imputation layer that leverages the soft cluster assignments across different views and the global cluster centroids to impute the missing views in a latent embedding space. However, the imputation procedure of missing views without the guidance of true data distributions inevitably introduces noise information

and consequentially reduces the quality of imputed views. As a result, the low-quality imputed views further degrade the learning process of the IMvC methods, leading to an under-optimal view-common representation for clustering.

Different from previous methods, we propose to cluster the incomplete multi-view data without the missing view imputation to avoid introducing inaccurate information. To achieve this goal, the following challenge needs to be addressed: *How can we reduce the impact of missing values across different views when merging information from multiple sources while learning a discriminative view-common feature representation for data clustering?* The missing views are difficult to be directly fused due to the missing values. Even some imputation manners are exploited to handle the missing views so that the multi-view features are easier to be aggregated, the uncontrollable information underlying the missing views contains inevitable adverse effects during the fusion process. Thus, it is emerging to design a flexible and effective multi-view fusion strategy to learn and integrate multi-view information when facing either complete or incomplete parts of the data. The final target of multi-view information fusion is to seek a view-common representation for clustering. The prior knowledge, e.g. the manifold structures (Meilă & Zhang, 2024) of different views, is valuable for representation learning since the prior knowledge helps to regularize the aggregated view-common feature representation with a compact and discriminative structure that polishes the noise information. Yet previous methods usually ignore utilizing such prior structural knowledge to boost the aggregated view-common features in the IMvC task.

Based on the above discussion, we propose Mask-IMvC (short for Mask-informed Deep Contrastive Incomplete Multi-view Clustering), a novel solution that flexibly and effectively integrates the information among incomplete multi-view data for clustering. As shown in Fig 1 (b), we first introduce a mask-informed fusion network that takes the observation status of samples across various views into consideration to formulate a mask, removing the contributions missing sample during the multi-view information aggregation. Afterward, a prior knowledge-assisted contrastive learning is designed, in which the neighbor correlations of each sample captured from different views are injected into the learned view-common representation with a re-weighted contrastive loss to achieve a more compact and clear cluster structure. As a result, the incomplete multi-view information is elegantly aggregated into a view-common feature representation for clustering. The contributions are summarized as follows,

- We propose Mask-IMvC which is a flexible and effective imputation-free framework to integrate comprehensive information from incomplete multi-view data

for clustering while reducing the adverse effects of missing values.

- We employ a re-weighted contrastive loss to regularize the view-common representation with a compact and clear cluster structure with the guidance of neighbor connection probabilities among samples across diverse views so as to boost the clustering performance.
- We perform extensive experiments on various benchmark multi-view datasets to verify the effectiveness of the Mask-IMvC method on both MvC and IMvC tasks.

2. Related Work

2.1. Incomplete Multi-view Clustering

Existing IMvC approaches can be generally grouped into: traditional IMvC methods (Wen et al., 2020a; Yin & Sun, 2021; Wang et al., 2022) and deep IMvC algorithms (Yang et al., 2022; Xu et al., 2024a; Yan et al., 2024).

Traditional IMvC methods commonly build upon matrix factorization, kernel learning, and graph learning technologies. Matrix factorization-based approaches derive a view-shared representation across diverse views via the matrix factorization techniques (Hu & Chen, 2019; Wen et al., 2024; Khan et al., 2024). For instance, an adaptive feature weighting manner is inserted into matrix factorization to mitigate the effects of redundant and noisy features on the learned view-shared representation, which is also regularized with a graph-embedded consensus constraint to preserve the structural information inherent in incomplete multi-view data. Kernel-based methods (Liu, 2024; Li et al., 2024a) utilizes a set of per-computed kernels to measure diverse views, tending to formulate a unified kernel through linear or non-linear combinations of predefined kernels to capture the clustering results. Liu et al. (Liu, 2024) jointly conduct incomplete kernel matrices imputation and alignment to capture an advanced clustering representation. Graph-based methods (Yang et al., 2024; Du et al., 2024; Li et al., 2022) integrate graph similarities captured from various views via either self-representation (Elhamifar & Vidal, 2013) or adaptive neighbor graph learning (Nie et al., 2014) manner, ultimately obtaining the clustering results through spectral clustering. Li et al. (Li et al., 2022) explored the cross-view information to refine the graph structure by leveraging the tensor nuclear norm. Deep learning-based methods (Wen et al., 2020b; Xu et al., 2022a; Li et al., 2023) leverage the powerful representation capabilities of deep neural networks to derive consensus clustering results from multi-view data. For example, Lin et al. (Lin et al., 2021) learned the consensus representation across diverse views by contrastive learning and recovered the missing views by cross-view prediction. Xue et al. (Xue et al., 2024) developed a multi-graph contrastive regularization to reduce abundant correlations

across multiple views and learn discriminative representations for clustering.

Previous IMvC methods have made significant strides in improving clustering performance following the main pipeline that imputes missing views and conducts clustering. However, the imputation procedure without the true data distributions inevitably causes inaccurate imputed missing views, which in turn degrade clustering performance. Different from them, we learn a view-common representation only from the observed parts of incomplete multi-view without the imputation procedure. To this end, we propose a mask-informed deep contrastive incomplete multi-view clustering method that reduces the impacts of missing values among different views on formulating a view-common representation from multiple views for clustering.

2.2. Contrastive Learning

Contrastive learning is a novel self-supervised learning paradigm that has achieved significant success across various computer vision and machine learning tasks (Krishnan et al., 2022; Liu et al., 2021b). Its core principle involves pushing samples away from their negative anchors while pulling samples closer to their positive anchors, thereby creating a discriminative representation for downstream tasks (Khosla et al., 2020). Over the past few years, different contrastive learning approaches have emerged, including MoCo (He et al., 2020), SimCLR (Chen et al., 2020), and SwAV (Caron et al., 2020). For a comprehensive overview of additional methods, we refer to the survey in (Gui et al., 2024).

Recently, inspired by the robust feature learning capabilities of self-supervised learning, contrastive loss has been extensively applied in MvC. For instance, Xu et al. (Xu et al., 2022b) aligned multi-view information from both high-level semantics and low-level features through contrastive learning, effectively capturing common semantics for clustering. Additionally, the work in (Trosten et al., 2023) explored the effectiveness of self-supervision and contrastive alignment within the multi-view clustering task. Luo et al. (Luo et al., 2024) first fused multi-view information at the data level and then applied data augmentation for the fused data, making a shared feature extractor with a simple contrastive learning paradigm to capture robust features for clustering. However, previous methods typically treat the same samples from different views as positive pairs, while diverse samples across multiple views are considered negative pairs. This manner lacks the flexibility to leverage sample connection probabilities to enhance feature representation learning. Thus, we propose prior knowledge-assisted contrastive learning to inject the sample connection probabilities from diverse views into the view-common feature representation with a carefully designed re-weighted contrastive loss. In such

a manner, the view-common feature representation full of structural information is beneficial for recovering the underlying cluster structure of data.

3. Methodology

In this section, we first provide the notations used in this paper. Then, we present the details of our proposed mask-informed deep contrastive incomplete multi-view clustering framework and prior knowledge-assisted contrastive learning.

3.1. Notation

In this paper, the IMvC data is denoted as $\{\mathbf{X}^v \in \mathbb{R}^{N \times D^v}\}_{v=1}^V$, where N and V are the number of samples and views, respectively. D^v represents the feature dimension of v -th view. A mask matrix $\mathbf{M} \in \mathbb{R}^{N \times V}$ restores the information that samples are observed or missing in specific views as,

$$m_{iv} = \begin{cases} 1 & \text{if } i\text{-th sample is observed in } v\text{-th view,} \\ 0 & \text{if } i\text{-th sample is absent in } v\text{-th view,} \end{cases} \quad (1)$$

where m_{iv} is the iv -th element of \mathbf{M} . Based on the mask \mathbf{M} , feature representations $\{\mathbf{X}^v\}_{v=1}^V$ can be divided into two parts, i.e. the observed parts $\{\bar{\mathbf{Z}}^v \in \mathbb{R}^{N_o^v \times D^v}\}_{v=1}^V$ and view missing parts $\{\hat{\mathbf{Z}}^v \in \mathbb{R}^{N_m^v \times D^v}\}_{v=1}^V$, where N_o^v and N_m^v denote the number of observed and absent samples in v -th view, respectively. In $\{\mathbf{X}^v\}_{v=1}^V$, the view missing parts $\{\hat{\mathbf{Z}}^v\}_{v=1}^V$ are unknown caused by some feature extraction failure cases. Note that when the mask \mathbf{M} is an all-ones matrix, the data is referred to as complete multi-view data; otherwise, it is incomplete multi-view data.

To transfer the observed parts $\{\bar{\mathbf{Z}}^v\}_{v=1}^V$ and view missing parts $\{\hat{\mathbf{Z}}^v\}_{v=1}^V$ back into the original sample orders in $\{\mathbf{X}^v\}_{v=1}^V$, we formulate two kinds of transition matrices, i.e. $\{\bar{\mathbf{T}}^v \in \mathbb{R}^{N_o^v \times N}\}_{v=1}^V$ and $\{\hat{\mathbf{T}}^v \in \mathbb{R}^{N_m^v \times N}\}_{v=1}^V$ as,

$$\bar{t}_{ij}^v = \begin{cases} 1 & \text{if } \bar{\mathbf{z}}_i^v \text{ is in the position of } \mathbf{x}_j^v, \\ 0 & \text{otherwise,} \end{cases} \quad (2)$$

$$\hat{t}_{ij}^v = \begin{cases} 1 & \text{if } \hat{\mathbf{z}}_i^v \text{ is in the position of } \mathbf{x}_j^v, \\ 0 & \text{otherwise,} \end{cases} \quad (3)$$

where \bar{t}_{ij}^v and \hat{t}_{ij}^v are the ij -th elements in $\bar{\mathbf{T}}^v$ and $\hat{\mathbf{T}}^v$, respectively. Based on them, we can permute the observed parts $\{\bar{\mathbf{Z}}^v\}_{v=1}^V$ and view missing parts $\{\hat{\mathbf{Z}}^v\}_{v=1}^V$ back into the original feature orders as,

$$\mathbf{X}^v = \bar{\mathbf{Z}}^v \bar{\mathbf{T}}^v + \hat{\mathbf{Z}}^v \hat{\mathbf{T}}^v \quad (4)$$

3.2. Overview

As shown in Fig. 2, our proposed mask-informed deep contrastive incomplete multi-view clustering framework con-

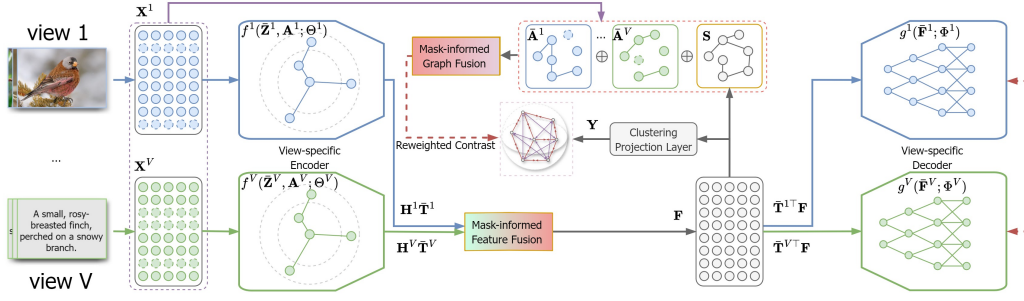


Figure 2. Illustration of mask-informed deep contrastive incomplete multi-view clustering (Mask-IMvC). The view-complete parts of IMvC data are first processed through their encoders to extract view-specific latent features. Next, a mask-informed fusion module aggregates the representations into a unified view-common one, which is then used to reconstruct the view complete parts of IMvC data via view-specific decoders. Finally, the prior knowledge from different views is fused via the mask-informed fusion strategy to assist the contrastive learning on the view-common representation.

sists of three parts, including view-specific encoders, decoders, and mask-informed fusion.

View-specific encoders: The graph convolutional networks (GCNs) are widely used in many data mining tasks, aggregating the neighbor information to learn features (Xia et al., 2021). In our method, we first construct k -nearest neighbor graphs $\{\mathbf{A}^v \in \mathbb{R}^{N_o^v \times N_o^v}\}_{v=1}^V$ from the observed parts $\{\bar{\mathbf{Z}}^v\}_{v=1}^V$ by the adaptive neighbor learning method (Nie et al., 2014). The view-specific encoders $\{f^v(\bar{\mathbf{Z}}^v, \mathbf{A}^v; \Theta^v)\}_{v=1}^V$, with Θ^v denoting the parameters, are implemented by several GCN layers to merge the neighbor information of each sample to learn view-specific latent representations. One of the GCN layers is formulated as follows,

$$\mathbf{H}^v = \sigma(\mathbf{D}^{v-\frac{1}{2}} \bar{\mathbf{A}}^v \mathbf{D}^{v-\frac{1}{2}} \mathbf{H}^v \mathbf{W}^v), \quad (5)$$

where $\mathbf{H}^v \in \mathbb{R}^{N \times L}$ is the v -th view latent representation. L denotes the feature dimension. $\bar{\mathbf{A}}^v = \mathbf{A}^v + \mathbf{I}$, with $\mathbf{I} \in \mathbb{R}^{N_o^v \times N_o^v}$ denoting an identity matrix. \mathbf{D}^v is a degree matrix of \mathbf{A}^v .

Mask-informed fusion: After the view-specific feature extraction, the obtained multiple features are permuted as the same orders as the original features as by transition matrices $\{\bar{\mathbf{T}}^v \in \mathbb{R}^{N_o^v \times N}\}_{v=1}^V$ as,

$$\bar{\mathbf{H}}^v = \mathbf{H}^v \bar{\mathbf{T}}^v. \quad (6)$$

The mask \mathbf{M} indicates whether there exist samples in specific views. Based on this knowledge, we exploit mask \mathbf{M} to filter the missing value and remove their contributions during the multi-view feature aggregation procedure as follows,

$$\mathbf{f}_i = \frac{\sum_{v=1}^V m_{iv} \bar{\mathbf{h}}_i^v}{\sum_{v=1}^V m_{iv}}, \quad (7)$$

where \mathbf{f}_i is the i -th samples of view-common features \mathbf{F} . In such an above manner, incomplete information is automatically filtered to avoid adverse impacts on the view-common

features. To further boost the representation capability of \mathbf{F} , we introduced a prior knowledge-assisted contrastive learning manner that is detailed depicted in Section 3.3.

View-specific decoders: The view-specific decoders are introduced to reconstruct the observed parts in the original IMvC data. To this end, we first obtain the observed parts of each view in the view-common feature \mathbf{F} by transition matrices $\{\bar{\mathbf{T}}^v\}_{v=1}^V$ as,

$$\bar{\mathbf{F}}^v = \bar{\mathbf{T}}^v \mathbf{F}, \quad (8)$$

where $\bar{\mathbf{F}}^v \in \mathbb{R}^{N_o^v \times L}$ is the obtained observed parts of each view in the view-common feature \mathbf{F} . Afterward, latent features pass to the view-specific decoders $\{g^v(\bar{\mathbf{F}}^v; \Phi^v)\}_{v=1}^V$ to reconstruct the view-specific features, which is optimized by minimizing the reconstruction loss between the original and reconstructed features as,

$$\ell_{rec} = \frac{1}{N} \sum_{v=1}^V \sum_{i=1}^{N_o^v} \|\bar{\mathbf{z}}_i^v - g^v(\bar{\mathbf{f}}_i^v; \Phi^v)\|_2^2. \quad (9)$$

3.3. Prior Knowledge-assisted Contrastive Learning

The similarities among samples defined from the original features are critical prior knowledge for feature representation learning (He & Niyogi, 2003). In this section, we inject the prior knowledge into the view-common feature representation with useful self-supervised contrastive learning to further boost its representation capability. To this end, we formulate three key components, i.e., the clustering projection layer, mask-informed graph fusion, and contrastive loss.

Clustering projection layer: In this part, we first transfer the view-common representation into the cluster space with a single linear layer. Then, the QR decomposition (Gander, 1980) is introduced to guarantee the orthogonal property of the clustering indicator matrix $\mathbf{Y} \in \mathbb{R}^{N \times C}$, where C is the

number of clusters. And the clustering distributions of the incomplete multi-view data can be revealed in \mathbf{Y} .

Mask-informed graph fusion: To flexibly merge multiple similarity graphs constructed from IMvC data, view-specific graphs $\{\mathbf{A}^v\}_{v=1}^V$ are first transferred based on transition matrices $\{\bar{\mathbf{T}}^v\}_{v=1}^V$ as,

$$\bar{\mathbf{A}}^v = \bar{\mathbf{T}}^{v\top} \mathbf{A}^v \bar{\mathbf{T}}^v, \quad (10)$$

where $\bar{\mathbf{A}}^v \in \mathbb{R}^{N \times N}$ is the transferred view-specific graph in v -view. Due to the incompleteness of data, $\{\bar{\mathbf{A}}^v\}_{v=1}^V$ only provides the sample similarities among the observed samples in each view, lacking the similarities among all samples. Thus, we construct a view-common similarity graph $\mathbf{S} \in \mathbb{R}^{N \times N}$ from view-common feature representation \mathbf{F} to measure the sample correlations among all points. Simply averaging the matrices to fuse the sample similarities from multiple graphs will bring in the noise information caused by the incomplete values. Thus, we utilize the mask \mathbf{M} to filter entries of missing values to achieve more effective fusion. To this end, the graph mask matrices $\{\mathbf{R}^v \in \mathbb{R}^{N \times N}\}_{v=1}^V$ is introduced based on the mask matrix \mathbf{M} to indicate whether there exists sample correlations in $\{\bar{\mathbf{A}}^v\}_{v=1}^V$, computed as,

$$r_{ij}^v = m_{iv} m_{jv}, \quad (11)$$

where r_{ij}^v is the ij -th element of \mathbf{R}^v . Finally, the comprehensive similarity information among multiple graphs can be merged as,

$$\hat{a}_{ij} = \frac{\sum_{v=1}^V r_{ij}^v \bar{a}_{ij}^v + s_{ij}}{\sum_{v=1}^V r_{ij}^v + 1}, \quad (12)$$

where \hat{a}_{ij} is the ij -th element of graph $\hat{\mathbf{A}} \in \mathbb{R}^{N \times N}$.

Contrastive loss: The contrastive learning approaches push the samples far away from the negative anchors while pulling in the samples with positive anchors (Chen et al., 2020; Wang & Liu, 2021). A straightforward way of constructing the positive and negative pairs is to leverage the sample connections in the graph $\hat{\mathbf{A}}$. Assuming that the neighbor points of each sample can be regarded as their positive anchors, and the points in the neighborhood of other samples can be treated as the negative anchors, we can construct the following contrastive loss to constrain the clustering distribution \mathbf{Y} as formulation of InfoNCE (Yeh et al., 2022) as ¹,

$$\zeta_{dcl} = -\frac{1}{N} \sum_{i=1}^N \log \frac{\sum_{j \in N^+} e^{\frac{\text{sim}(\mathbf{y}_i, \mathbf{y}_j)}{\tau}}}{\sum_{r \in N^-} e^{\frac{\text{sim}(\mathbf{y}_i, \mathbf{y}_r)}{\tau}}}, \quad (13)$$

¹The positive part is removed from denominator to alleviate the negative-positive-coupling issue.

where $\text{sim}(\mathbf{y}_i, \mathbf{y}_j)$ denotes the cosine similarity computed as $\mathbf{y}_i \mathbf{y}_j^\top / \|\mathbf{y}_i\| \|\mathbf{y}_j\|$. τ is a temperature parameter. N^+ and N^- respectively denote the positive and negative sets defined by sample connection relationships of the graph $\hat{\mathbf{A}}$.

Similarity graph $\hat{\mathbf{A}}$ measures similarities of samples as their connection possibilities in the range of $[0, 1]$ as defined in (Nie et al., 2014). Simply treating the two samples with connection possibility \hat{a}_{ij} larger than 0 as the positive pair is not suitable due to there is also $1 - \hat{a}_{ij}$ possibility that can be regarded as negative pair. Therefore, we can further re-weight the Eq. (13) from a binary case into continual version as,

$$\zeta_{wcl} = -\frac{1}{N} \sum_{i=1}^N \log \frac{\sum_{j=1}^N \hat{a}_{ij} e^{\frac{\text{sim}(\mathbf{y}_i, \mathbf{y}_j)}{\tau}}}{\sum_{r=1}^N (1 - \hat{a}_{ir}) e^{\frac{\text{sim}(\mathbf{y}_i, \mathbf{y}_r)}{\tau}}}. \quad (14)$$

As shown in Eq. (14), the positive and negative pairs can be adaptively determined by the similarity graph $\hat{\mathbf{A}}$. In addition, the samples with similarities equal to zeros are automatically treated as negative pairs. The samples with similarities larger than zeros ensure the possibility of being grouped into either positive or negative pairs that are re-weighted with their corresponding possibilities. Under this contrastive loss, the view-common feature representation preserves the neighbor information among different samples and reveals more compact and clear structures for clustering.

3.4. Total Loss Function

Finally, the total loss function of the proposed model is formulated as,

$$\mathcal{L} = \ell_{rec} + \lambda \zeta_{wcl} \quad (15)$$

where λ is a hyper-parameter to balance reconstruction loss ℓ_{rec} and re-weighted contrastive loss ζ_{wcl} .

4. Experiments

4.1. Experimental Settings

Datasets: In our experiments, we evaluate our proposed method on eight widely used multi-view datasets, including MSRCV ², CUB ³, OutdoorScene (Hu et al., 2020), and nuswide (Zhen et al., 2019). The details descriptions of the datasets are given in the appendix.

Evaluation metrics: Four widely used evaluation metrics, i.e., accuracy (ACC), normalized mutual information (NMI), adjusted Rand index (ARI), and Fscore are utilized to evaluate the clustering performance. And higher value of each metric denotes a better clustering result.

²<https://mldta.com/dataset/msrc-v1/>

³<https://www.vision.caltech.edu/visipedia/CUB-200.html>

Mask-informed Deep Contrastive Incomplete Multi-view Clustering

Table 1. The clustering performance measured by ACC, NMI, ARI, and Fscore of all compared methods on multi-view datasets. The highest and the second highest values under each metric are **bolded** and underlined, respectively.

Datasets	CUB				MSRCV				OutdoorScene				nuswide			
Methods	ACC	NMI	ARI	Fscore	ACC	NMI	ARI	Fscore	ACC	NMI	ARI	Fscore	ACC	NMI	ARI	Fscore
DCCA	60.09	55.87	40.79	48.84	68.90	62.09	50.06	61.84	48.16	51.58	36.42	49.76	48.16	40.03	22.89	41.40
AWP	81.17	75.20	65.52	69.00	67.62	62.16	53.58	60.23	60.83	45.51	37.37	45.98	55.93	47.05	36.38	44.37
GMC	79.50	78.95	66.48	70.03	73.81	74.32	64.03	69.41	33.56	42.33	18.78	35.02	22.83	19.60	1.72	19.68
OPMC	71.50	75.67	60.92	64.95	82.38	73.38	66.96	71.63	63.17	51.57	42.22	49.62	58.60	44.87	37.35	43.82
MFLVC	67.00	62.91	49.24	55.59	63.33	55.42	45.23	57.13	64.62	55.15	42.90	51.11	32.10	20.75	16.09	24.40
DealMVC	61.00	66.10	51.27	58.04	44.29	31.91	19.54	37.77	<u>75.26</u>	62.73	54.21	61.83	51.93	37.88	32.75	38.81
CVCL	79.33	71.03	61.54	66.17	72.00	58.60	50.23	59.08	71.65	60.23	50.34	57.98	58.63	<u>48.30</u>	<u>39.92</u>	<u>47.41</u>
EEOMVC	65.00	66.49	51.32	56.43	69.05	54.64	45.63	53.30	57.70	40.35	29.64	39.02	<u>61.27</u>	45.02	39.80	46.09
SCMVC	72.83	68.71	55.82	61.66	71.90	63.02	56.26	63.36	72.10	60.57	52.56	59.89	53.97	40.63	34.91	41.37
SCM	84.83	<u>79.11</u>	<u>71.23</u>	<u>75.17</u>	<u>89.05</u>	<u>80.95</u>	<u>76.66</u>	<u>81.01</u>	60.45	51.95	41.59	49.93	57.63	44.17	38.51	44.56
Ours	<u>81.98</u>	85.33	76.23	81.97	90.76	81.84	79.28	83.37	75.53	<u>61.19</u>	<u>54.13</u>	<u>61.54</u>	64.34	49.89	41.33	50.32

Table 2. The clustering performance measured by ACC, NMI, ARI, and Fscore of all compared methods on multi-view datasets with different missing rates η . The highest and the second highest values under each metric are **bolded** and underlined, respectively.

η	Datasets	CUB				MSRCV				OutdoorScene				nuswide			
	Methods	ACC	NMI	ARI	Fscore	ACC	NMI	ARI	Fscore	ACC	NMI	ARI	Fscore	ACC	NMI	ARI	Fscore
0.10	EFAE	64.94	64.84	51.83	59.76	70.35	59.67	51.94	60.55	63.15	51.26	42.65	51.83	51.69	37.06	29.97	38.80
	MFAE	62.35	64.65	51.14	58.52	66.11	58.03	49.16	59.30	62.31	50.74	41.33	50.53	53.61	41.14	33.41	<u>42.07</u>
	DCCA	33.01	28.50	11.02	29.80	46.69	38.94	21.14	44.58	50.01	49.53	34.41	47.58	34.51	24.30	10.78	31.46
	DSIMVC	56.07	56.31	38.85	45.66	47.62	38.88	28.21	39.34	54.99	50.76	35.87	44.23	33.57	25.19	16.53	24.86
	DSIMVC++	59.70	57.25	41.07	47.52	44.76	37.65	24.85	36.85	54.89	49.23	35.27	43.63	41.32	35.12	24.15	31.58
	CPSPAN	63.37	62.80	48.18	60.86	73.43	66.40	56.24	70.87	57.96	49.55	37.15	<u>57.83</u>	39.47	28.74	19.00	39.25
	GIGA	73.77	77.54	63.42	<u>71.96</u>	74.48	<u>76.69</u>	<u>62.52</u>	<u>76.14</u>	46.57	54.58	35.13	52.72	30.61	30.54	7.18	41.01
	MVCAN	60.34	62.40	49.09	56.36	65.75	55.97	46.67	57.46	<u>65.50</u>	<u>56.62</u>	<u>46.39</u>	54.68	49.05	36.51	28.85	37.44
	SCM	79.37	73.75	<u>64.10</u>	69.01	<u>76.95</u>	67.85	60.35	67.63	59.73	48.46	37.72	47.26	<u>56.43</u>	<u>41.29</u>	<u>34.69</u>	41.80
Ours	<u>78.95</u>	<u>77.31</u>	65.62	72.37	89.69	80.01	77.20	81.63	74.20	61.62	51.96	61.04	60.67	46.15	39.64	46.74	
0.30	EFAE	46.39	49.34	31.34	41.60	58.98	47.63	38.47	48.98	55.01	43.38	35.83	45.27	41.30	29.18	19.68	29.91
	MFAE	46.24	49.07	30.93	40.81	55.01	45.29	35.56	46.83	48.79	39.34	32.23	41.24	41.45	31.16	20.84	30.93
	DCCA	19.31	12.90	1.83	24.31	22.10	12.65	1.51	31.81	49.99	46.92	32.27	45.53	20.31	7.42	1.79	20.15
	DSIMVC	53.13	51.93	34.17	41.58	44.10	38.57	26.56	38.50	52.89	48.83	33.50	42.18	26.55	17.37	11.16	21.16
	DSIMVC++	61.77	58.04	42.58	48.88	52.10	43.77	32.54	42.97	53.92	48.83	34.42	42.78	45.41	<u>37.04</u>	<u>26.84</u>	34.22
	CPSPAN	60.37	59.56	43.70	59.62	71.24	65.47	54.22	68.34	56.05	48.13	35.32	<u>56.02</u>	39.67	28.63	19.44	<u>39.25</u>
	GIGA	<u>71.47</u>	74.48	60.16	69.15	70.76	73.16	56.96	<u>72.55</u>	43.65	<u>49.82</u>	28.52	51.73	28.57	26.90	6.15	38.33
	MVCAN	49.23	49.77	33.66	42.41	47.17	36.39	26.68	39.37	51.67	45.57	35.23	44.10	37.12	26.24	16.90	27.65
	SCM	68.63	63.79	50.93	58.65	<u>80.10</u>	66.44	<u>60.54</u>	67.77	<u>59.51</u>	47.66	<u>36.72</u>	46.29	<u>47.21</u>	33.45	24.57	33.75
Ours	73.91	<u>71.60</u>	<u>57.89</u>	<u>66.94</u>	82.62	<u>72.31</u>	65.80	73.09	67.58	56.93	46.71	57.22	53.33	40.48	28.82	40.21	
0.50	EFAE	37.11	40.26	17.33	32.59	48.29	38.13	26.97	40.02	48.69	37.15	28.48	38.64	28.95	21.22	9.41	23.05
	MFAE	37.80	41.23	18.41	32.78	45.95	33.73	22.31	36.63	40.14	29.92	22.45	32.39	31.17	24.91	11.45	25.24
	DCCA	14.01	5.30	0.29	20.23	19.08	7.44	0.71	28.58	47.49	42.76	29.95	42.57	14.24	2.17	0.18	18.11
	DSIMVC	52.82	51.70	34.07	41.55	43.52	35.45	23.34	36.06	52.98	47.91	32.92	41.81	27.78	17.24	11.54	21.24
	DSIMVC++	60.30	56.93	40.83	47.29	47.33	38.09	26.60	38.28	52.37	47.10	32.94	41.45	<u>42.70</u>	34.24	24.45	31.68
	CPSPAN	61.27	61.52	45.93	59.29	70.09	62.06	50.84	67.23	56.98	47.45	35.47	56.83	42.64	30.34	<u>21.81</u>	42.53
	GIGA	69.30	70.35	54.35	64.85	72.19	70.13	<u>54.00</u>	70.11	48.57	54.97	34.06	<u>54.36</u>	33.51	30.91	7.23	<u>41.37</u>
	MVCAN	37.69	42.19	21.38	31.93	38.13	25.14	15.08	30.25	42.61	35.92	26.45	36.10	30.59	21.02	10.17	23.83
	SCM	61.83	59.83	45.41	52.21	<u>73.71</u>	58.33	50.30	59.84	<u>59.19</u>	48.32	<u>38.49</u>	47.36	41.76	28.57	15.88	29.80
Ours	<u>68.46</u>	<u>68.39</u>	<u>52.74</u>	<u>63.05</u>	80.25	<u>69.42</u>	60.73	<u>70.08</u>	60.84	<u>49.47</u>	38.51	50.19	45.51	<u>34.12</u>	19.13	34.96	

4.2. Experimental Results

To verify the effectiveness of the proposed method, we perform experiments on both view-complete and view-missing settings with various approaches. The detailed results and analysis are given in the following parts.

Results on complete MvC datasets: In this part, we com-

pared the proposed method on view-complete MvC datasets with ten different approaches, including DCCA (Wang et al., 2015), AWP (Nie et al., 2018), GMC (Wang et al., 2020), OPMC (Liu et al., 2021a), MFLVC (Xu et al., 2022b), DealMVC (Chen et al., 2023), CVCL (Chen et al., 2023), EEOMVC (Wang et al., 2023a), SCMVC (Wu et al., 2024) and SCM (Luo et al., 2024). The parameters in all com-

pared approaches are tuned with a grid search scheme as suggested in their papers to implement their best clustering performance. In Tab. 1, we present the clustering results in terms of four metrics on four MvC datasets of all methods.

From the Tab. 1, we obtain the following observations: Our method consistently performs better than other competitors on four datasets. For example, the proposed method outperforms the second performer, e.g. SCM method, with about 1.71, 0.98, 2.62, and 2.36 percentages in terms of ACC, NMI, ARI, and Fscore on the MSRCV dataset. Such advantages can be observed consistently on other datasets, which indicates the superiority of the proposed method. There are some methods, e.g. MFLVC, DealMVC, CVCL, and SCM, built upon contrastive learning. They usually treat the sample samples in different views as the positive pairs, while formulating the different samples in diverse views as the negative pairs. This type of contrastive learning manner inevitably ignores the structural information among multi-view datasets, resulting in sub-optimal clustering performance. Differently, the proposed method constructs the positive and negative pairs based on the similarities among different samples and further introduces a weighted contrastive loss to guide the model to learn more discriminative view-common feature representation for clustering. The deep MvC methods, e.g., Ours, SCM, and SCMVC perform better than traditional MvC approaches, e.g. AWP, GMC, and OPMC, demonstrating the effectiveness of deep feature representation. The above superior performance of the proposed method strongly verifies the effectiveness of the proposed method.

Results on incomplete MvC datasets: We verify the superiority of the proposed method on incomplete MvC datasets with nine different approaches: EEAE, MFAE, DCCA (Wang et al., 2015), DSIMVC (Tang & Liu, 2022), DSIMVC++ (Yan et al., 2023), CPSPAN (Jin et al., 2023), GIGA (Yang et al., 2024), MVCAN (Xu et al., 2024b) and SCM (Luo et al., 2024). The parameters in all compared approaches are tuned with a grid search scheme as suggested in their papers to implement their best clustering performance. In our experiments, we follow the strategy used in (Chen et al., 2023) to transfer the view-complete MvC data into view-complete settings with the missing rate η in the range of [0.1, 0.3, 0.5]. In Tab. 2, we present the clustering results in terms of four metrics on four MvC datasets of all methods with missing rates varying from 0.1 to 0.5.

From the Tab. 2, we obtain the following observations: The proposed method achieves better clustering results than other compared approaches on different datasets with diverse missing rates. For example, our method performs better than the second-best results about 8.71, 3.11, 9.99, and 1.2 percentages measured by ACC, NMI, ARI, and Fscore on the OutdoorScene dataset. Such clustering per-

formance advantages strongly indicate the effectiveness and superiority of the proposed method, which introduces a mask-informed fusion framework with a prior knowledge-assisted contrastive learning manner. The CPSPAN method imputes the view-specific latent features based on the cross-view similarity graph, which is used to find the nearest neighbor to fill missing samples. However, the imputation procedure without the true labels inevitably causes inaccurate missing view imputation, and consequentially degrades the final clustering results. GIGA and the proposed method are both imputation-free kind of approaches, which obtain better clustering results than the CPSPAN method. The MVCAN and SCM are originally designed for view-complete MvC datasets. In our experiments, we directly fill the missing samples with zeros and input MVCAN and SCM to get the clustering results. As seen from the results, MVCAN and SCM can still obtain consideration clustering performance compared with other well-designed incomplete MvC approaches in small missing ratios. The proposed method consistently performs better than MVCAN and SCM on different datasets with diverse missing ratio settings. This indicates that effectively leveraging the observation status of different samples across multiple views is beneficial for aggregating the information from IMvC data.

4.3. Model Analysis

In this section, we conduct a series of experiments to analyze the effectiveness of diverse components and different settings in the proposed method.

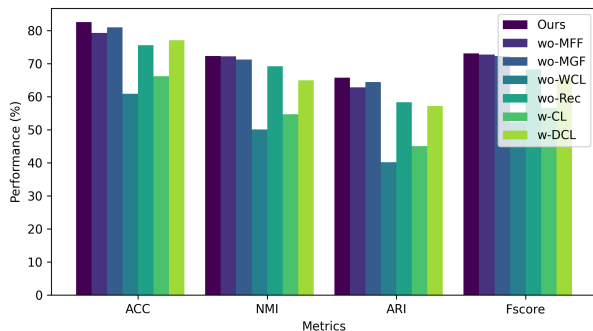


Figure 3. The ablation studies results of the proposed method on MSRCV dataset.

Effectiveness of mask-informed fusion strategy: The mask-informed fusion strategy consists of two parts, i.e., the mask-informed feature fusion and mask-informed graph fusion, which are utilized to aggregate the incomplete multi-view information with the help of data observation status across different views. Here, we formulate two methods called wo-MFF and wo-MGF, which remove the mask-informed feature fusion and mask-informed graph fusion from the model, respectively. Due to the limited space, we only report the comparison results on MSRCV datasets

in Fig. 3, and more comparison results on other datasets can be obtained in the appendix. As shown in Fig. 3, the clustering performance of the proposed method consistently outperforms than wo-MFF and wo-MGF methods, indicating the effectiveness of the proposed mask-informed fusion strategy.

Effectiveness of prior knowledge-assisted contrastive learning: The prior knowledge-assisted contrastive learning is a key component of the proposed method, which leverages the neighbor information captured from diverse views to boost the learning process of the view-common feature representation for clustering with a weighted contrastive loss. To study its effectiveness, we first remove the prior knowledge-assisted contrastive learning from our model and call it wo-WCL. As shown in Fig. 3, the clustering performance of the wo-WCL method significantly drops compared to the proposed model. In addition, we evaluate the clustering performance of the proposed model with only the prior knowledge-assisted contrastive loss without the feature reconstruction part and term it the wo-Rec method. From the results in Fig. 3, we observe that only with the prior knowledge-assisted contrastive loss can not achieve that optimal clustering performance. Thus, the feature reconstruction and prior knowledge-assisted contrastive learning are both important for the feature representation learning in the proposed method. Finally, we compare our weighted contrastive loss with the widely used contrastive loss (Chen et al., 2020) and decoupled contrastive loss (Yeh et al., 2022), which are marked as w-CL and w-DCL methods in Fig. 3. From the results, we find that 1) our weighted contrastive loss performs better than contrastive loss and decoupled contrastive loss in most cases, which indicates the weighted contrastive loss is suitable to utilize the prior knowledge of the incomplete multi-view data. 2) The weighted contrastive loss and decoupled contrastive loss achieve better results than contrastive loss indicating that the weighted contrastive loss and decoupled contrastive loss are less sensitive to the negative-positive-coupling issues (Yeh et al., 2022).

Parameter sensitivity analysis: Our proposed BMvC method consists of a key balance parameter λ to trade-off the feature reconstruction and view-specific contrastive regularization loss. To study the parameter sensitivity, we give the clustering performance measured by ACC, NMI, ARI, and Fscore on the nuswide dataset varying with different λ in Fig. 4a, and more results are given in the appendix. From the results, we observe that the clustering performance of the proposed method slightly fluctuates with the λ . Additionally, when the parameter λ is in the range $[10^{-1}, 10^0, 10^1]$, the proposed method obtains considerable clustering results. Therefore, we suggest setting the parameter λ in range $[10^{-1}, 10^0, 10^1]$, when it is applied for some applications.

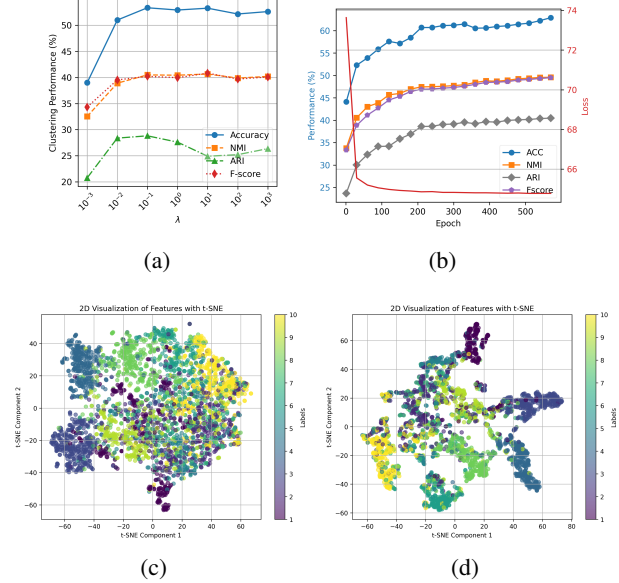


Figure 4. (a) The parameter sensitivity of the proposed method on nuswide dataset in terms of ACC, NMI, ARI, and Fscore, respectively. (b) the convergence analysis results on nuswide dataset. (c)-(d) the visualization results of the proposed method on nuswide dataset on epochs 1 and 200.

Convergence analysis and visualization: In this part, we report the clustering performance and loss function values varying from training epochs in Fig. 4b. The proposed method ensures good convergence properties. Additionally, we visualize the data distribution of the view-common feature presentation under different training epochs in Figs. 4c-4d. From the results, we find that the proposed method can reveal more compact and clear clustering results with the training epochs increase. More convergence and visualization results can be obtained in the appendix.

5. Conclusions

In this paper, we proposed a novel incomplete multi-view clustering method equipped with a mask-informed fusion strategy and prior knowledge-assisted contrastive learning. The mask-informed fusion strategy flexibly aggregates incomplete multi-view information by considering the data observation status across multiple views, reducing the adverse impacts of missing values. The prior knowledge-assisted contrastive learning leverages the neighbor information among different views to enhance the view-common feature representation with a weighted contrastive loss. Finally, Extensive experiments on various benchmark multi-view clustering datasets on both view complete and incomplete cases were conducted to verify the efficacy of our method.

References

- Caron, M., Misra, I., Mairal, J., Goyal, P., Bojanowski, P., and Joulin, A. Unsupervised learning of visual features by contrasting cluster assignments. *Advances in Neural Information Processing Systems*, 33:9912–9924, 2020.
- Chen, J., Mao, H., Woo, W. L., and Peng, X. Deep multiview clustering by contrasting cluster assignments. In *IEEE Conference on Computer Vision and Pattern Recognition*, pp. 16752–16761, 2023.
- Chen, T., Kornblith, S., Norouzi, M., and Hinton, G. A simple framework for contrastive learning of visual representations. In *International Conference on Machine Learning*, pp. 1597–1607. PMLR, 2020.
- Du, L., Shi, Y., Chen, Y., Zhou, P., and Qian, Y. Fast and scalable incomplete multi-view clustering with duality optimal graph filtering. In *ACM International Conference on Multimedia*, pp. 8893–8902, 2024.
- Elhamifar, E. and Vidal, R. Sparse subspace clustering: Algorithm, theory, and applications. *IEEE Transactions on Pattern Analysis and Machine Intelligence*, 35(11): 2765–2781, 2013.
- Gander, W. Algorithms for the qr decomposition. *Res. Rep.*, 80(02):1251–1268, 1980.
- Gui, J., Chen, T., Zhang, J., Cao, Q., Sun, Z., Luo, H., and Tao, D. A survey on self-supervised learning: Algorithms, applications, and future trends. *IEEE Transactions on Pattern Analysis and Machine Intelligence*, 2024.
- He, K., Fan, H., Wu, Y., Xie, S., and Girshick, R. Momentum contrast for unsupervised visual representation learning. In *IEEE/CVF conference on Computer Vision and Pattern Recognition*, pp. 9729–9738, 2020.
- He, X. and Niyogi, P. Locality preserving projections. *Advances in Neural Information Processing Systems*, 16, 2003.
- Hu, M. and Chen, S. One-pass incomplete multi-view clustering. In *AAAI Conference on Artificial Intelligence*, volume 33, pp. 3838–3845, 2019.
- Hu, Z., Nie, F., Wang, R., and Li, X. Multi-view spectral clustering via integrating nonnegative embedding and spectral embedding. *Information Fusion*, 55:251–259, 2020.
- Jin, J., Wang, S., Dong, Z., Liu, X., and Zhu, E. Deep incomplete multi-view clustering with cross-view partial sample and prototype alignment. In *IEEE/CVF Conference on Computer Vision and Pattern Recognition*, pp. 11600–11609, 2023.
- Khan, G. A., Khan, J., Anwar, T., Ashraf, Z., Javed, M. H., and Diallo, B. Weighted concept factorization based incomplete multi-view clustering. *IEEE Transactions on Artificial Intelligence*, 2024.
- Khosla, P., Teterwak, P., Wang, C., Sarna, A., Tian, Y., Isola, P., Maschinot, A., Liu, C., and Krishnan, D. Supervised contrastive learning. *Advances in Neural Information Processing Systems*, 33:18661–18673, 2020.
- Kingma, D. P. Adam: A method for stochastic optimization. *arXiv preprint arXiv:1412.6980*, 2014.
- Krishnan, R., Rajpurkar, P., and Topol, E. J. Self-supervised learning in medicine and healthcare. *Nature Biomedical Engineering*, 6(12):1346–1352, 2022.
- Li, A., Feng, C., Cheng, Y., Zhang, Y., and Yang, H. Incomplete multiview subspace clustering based on multiple kernel low-redundant representation learning. *Information Fusion*, 103:102086, 2024a.
- Li, H., Li, Y., Yang, M., Hu, P., Peng, D., and Peng, X. Incomplete multi-view clustering via prototype-based imputation. In *International Joint Conference on Artificial Intelligence*, pp. 3911–3919, 2023.
- Li, K., Wang, Y., He, Y., Li, Y., Wang, Y., Liu, Y., Wang, Z., Xu, J., Chen, G., Luo, P., et al. Mvbench: A comprehensive multi-modal video understanding benchmark. In *IEEE Conference on Computer Vision and Pattern Recognition*, pp. 22195–22206, 2024b.
- Li, X.-L., Chen, M.-S., Wang, C.-D., and Lai, J.-H. Refining graph structure for incomplete multi-view clustering. *IEEE Transactions on Neural Networks and Learning Systems*, 35(2):2300–2313, 2022.
- Lin, Y., Gou, Y., Liu, Z., Li, B., Lv, J., and Peng, X. Completer: Incomplete multi-view clustering via contrastive prediction. In *IEEE Conference on Computer Vision and Pattern Recognition*, pp. 11174–11183, 2021.
- Liu, J., Liu, X., Yang, Y., Liu, L., Wang, S., Liang, W., and Shi, J. One-pass multi-view clustering for large-scale data. In *International Conference on Computer Vision*, pp. 12344–12353, 2021a.
- Liu, X. Incomplete multiple kernel alignment maximization for clustering. *IEEE Transactions on Pattern Analysis and Machine Intelligence*, 46(3):1412–1424, 2024.
- Liu, X., Zhang, F., Hou, Z., Mian, L., Wang, Z., Zhang, J., and Tang, J. Self-supervised learning: Generative or contrastive. *IEEE Transactions on Knowledge and Data Engineering*, 35(1):857–876, 2021b.

- Luo, C., Xu, J., Ren, Y., Ma, J., and Zhu, X. Simple contrastive multi-view clustering with data-level fusion. In *International Joint Conference on Artificial Intelligence*, pp. 4697–4705, 2024.
- Meilä, M. and Zhang, H. Manifold learning: What, how, and why. *Annual Review of Statistics and Its Application*, 11, 2024.
- Nie, F., Wang, X., and Huang, H. Clustering and projected clustering with adaptive neighbors. In *International Conference on Knowledge Discovery and Data Mining*, pp. 977–986, 2014.
- Nie, F., Tian, L., and Li, X. Multiview clustering via adaptively weighted procrustes. In *International Conference on Knowledge Discovery and Data Mining*, pp. 2022–2030, 2018.
- Paszke, A., Gross, S., Massa, F., Lerer, A., Bradbury, J., Chanan, G., Killeen, T., Lin, Z., Gimelshein, N., Antiga, L., et al. Pytorch: An imperative style, high-performance deep learning library. *Advances in Neural Information Processing Systems*, 32, 2019.
- Pu, J., Cui, C., Chen, X., Ren, Y., Pu, X., Hao, Z., Philip, S. Y., and He, L. Adaptive feature imputation with latent graph for deep incomplete multi-view clustering. In *AAAI Conference on Artificial Intelligence*, volume 38, pp. 14633–14641, 2024.
- Schiappa, M. C., Rawat, Y. S., and Shah, M. Self-supervised learning for videos: A survey. *ACM Computing Surveys*, 55(13s):1–37, 2023.
- Tang, H. and Liu, Y. Deep safe incomplete multi-view clustering: Theorem and algorithm. In *International Conference on Machine Learning*, pp. 21090–21110. PMLR, 2022.
- Trosten, D. J., Løkse, S., Jenssen, R., and Kampffmeyer, M. C. On the effects of self-supervision and contrastive alignment in deep multi-view clustering. In *IEEE Conference on Computer Vision and Pattern Recognition*, pp. 23976–23985, 2023.
- Wang, F. and Liu, H. Understanding the behaviour of contrastive loss. In *IEEE Conference on Computer Vision and Pattern Recognition*, pp. 2495–2504, 2021.
- Wang, H., Yang, Y., and Liu, B. Gmc: Graph-based multi-view clustering. *IEEE Transactions on Knowledge and Data Engineering*, 32(6):1116–1129, 2020.
- Wang, J., Tang, C., Wan, Z., Zhang, W., Sun, K., and Zomaya, A. Y. Efficient and effective one-step multi-view clustering. *IEEE Transactions on Neural Networks and Learning Systems*, 2023a.
- Wang, S., Liu, X., Liu, L., Tu, W., Zhu, X., Liu, J., Zhou, S., and Zhu, E. Highly-efficient incomplete large-scale multi-view clustering with consensus bipartite graph. In *IEEE/CVF Conference on Computer Vision and Pattern Recognition*, pp. 9776–9785, 2022.
- Wang, W., Arora, R., Livescu, K., and Bilmes, J. On deep multi-view representation learning. In *International Conference on Machine Learning*, pp. 1083–1092. PMLR, 2015.
- Wang, X., Chen, G., Qian, G., Gao, P., Wei, X.-Y., Wang, Y., Tian, Y., and Gao, W. Large-scale multi-modal pre-trained models: A comprehensive survey. *Machine Intelligence Research*, 20(4):447–482, 2023b.
- Wang, Y. Survey on deep multi-modal data analytics: Collaboration, rivalry, and fusion. *ACM Transactions on Multimedia Computing, Communications, and Applications*, 17(1s):1–25, 2021.
- Wen, J., Yan, K., Zhang, Z., Xu, Y., Wang, J., Fei, L., and Zhang, B. Adaptive graph completion based incomplete multi-view clustering. *IEEE Transactions on Multimedia*, 23:2493–2504, 2020a.
- Wen, J., Zhang, Z., Zhang, Z., Wu, Z., Fei, L., Xu, Y., and Zhang, B. Dimc-net: Deep incomplete multi-view clustering network. In *ACM International Conference on Multimedia*, pp. 3753–3761, 2020b.
- Wen, J., Xu, G., Tang, Z., Wang, W., Fei, L., and Xu, Y. Graph regularized and feature aware matrix factorization for robust incomplete multi-view clustering. *IEEE Transactions on Circuits and Systems for Video Technology*, 34(5):3728–3741, 2024. doi: 10.1109/TCSVT.2023.3317877.
- Wu, S., Zheng, Y., Ren, Y., He, J., Pu, X., Huang, S., Hao, Z., and He, L. Self-weighted contrastive fusion for deep multi-view clustering. *IEEE Transactions on Multimedia*, 2024.
- Xia, F., Sun, K., Yu, S., Aziz, A., Wan, L., Pan, S., and Liu, H. Graph learning: A survey. *IEEE Transactions on Artificial Intelligence*, 2(2):109–127, 2021.
- Xu, G., Wen, J., Liu, C., Hu, B., Liu, Y., Fei, L., and Wang, W. Deep variational incomplete multi-view clustering: Exploring shared clustering structures. In *AAAI Conference on Artificial Intelligence*, volume 38, pp. 16147–16155, 2024a.
- Xu, J., Li, C., Ren, Y., Peng, L., Mo, Y., Shi, X., and Zhu, X. Deep incomplete multi-view clustering via mining cluster complementarity. In *AAAI Conference on Artificial Intelligence*, volume 36, pp. 8761–8769, 2022a.

- Xu, J., Tang, H., Ren, Y., Peng, L., Zhu, X., and He, L. Multi-level feature learning for contrastive multi-view clustering. In *IEEE Conference on Computer Vision and Pattern Recognition*, pp. 16051–16060, 2022b.
- Xu, J., Ren, Y., Wang, X., Feng, L., Zhang, Z., Niu, G., and Zhu, X. Investigating and mitigating the side effects of noisy views for self-supervised clustering algorithms in practical multi-view scenarios. In *IEEE Conference on Computer Vision and Pattern Recognition*, pp. 22957–22966, 2024b.
- Xue, Z., Li, Y., Guan, Z., Li, W., Liang, M., and Zhou, H. Robust multi-graph contrastive network for incomplete multi-view clustering. *IEEE Transactions on Multimedia*, 2024.
- Yan, W., Zhang, Y., Lv, C., Tang, C., Yue, G., Liao, L., and Lin, W. Gcfagg: Global and cross-view feature aggregation for multi-view clustering. In *IEEE/CVF Conference on Computer Vision and Pattern Recognition*, pp. 19863–19872, June 2023.
- Yan, W., Liu, K., Zhou, W., and Tang, C. Deep incomplete multi-view clustering via dynamic imputation and triple alignment with dual optimization. *IEEE Transactions on Circuits and Systems for Video Technology*, 2024.
- Yang, M., Li, Y., Hu, P., Bai, J., Lv, J., and Peng, X. Robust multi-view clustering with incomplete information. *IEEE Transactions on Pattern Analysis and Machine Intelligence*, 45(1):1055–1069, 2022.
- Yang, Z., Zhang, H., Wei, Y., Wang, Z., Nie, F., and Hu, D. Geometric-inspired graph-based incomplete multi-view clustering. *Pattern Recognition*, 147:110082, 2024.
- Yeh, C.-H., Hong, C.-Y., Hsu, Y.-C., Liu, T.-L., Chen, Y., and LeCun, Y. Decoupled contrastive learning. In *European Conference on Computer Vision*, pp. 668–684. Springer, 2022.
- Yin, J. and Sun, S. Incomplete multi-view clustering with reconstructed views. *IEEE Transactions on Knowledge and Data Engineering*, 35(3):2671–2682, 2021.
- Zhen, L., Hu, P., Wang, X., and Peng, D. Deep supervised cross-modal retrieval. In *IEEE Conference on Computer Vision and Pattern Recognition*, pp. 10394–10403, 2019.
- Zhou, L., Du, G., Lü, K., Wang, L., and Du, J. A survey and an empirical evaluation of multi-view clustering approaches. *ACM Computing Surveys*, 56(7):1–38, 2024.
- Zou, X., Tang, C., Zheng, X., Li, Z., He, X., An, S., and Liu, X. Dpnet: Dynamic poly-attention network for trustworthy multi-modal classification. In *Proceedings of the 31st ACM International Conference on Multimedia*, pp. 3550–3559, 2023.
- Zou, X., Wang, Y., Yan, Y., Huang, S., Zheng, K., Chen, J., Tang, C., and Hu, X. Look twice before you answer: Memory-space visual retracing for hallucination mitigation in multimodal large language models. *arXiv preprint arXiv:2410.03577*, 2024.

A. More Results for Model Analysis

A.1. Effectiveness of mask-informed fusion strategy and prior knowledge-assisted contrastive learning

The ablation study of the proposed method in terms of ACC, NMI, ARI, and Fscore on four benchmark multi-view datasets with missing rate $\eta = 0.3$ are given in Tab. 3.

Table 3. The ablation study of the proposed method in terms of ACC, NMI, ARI, and Fscore on four benchmark multi-view datasets.

Datasets	CUB				MSRCV				OutdoorScene				nuswide			
Methods	ACC	NMI	ARI	Fscore	ACC	NMI	ARI	Fscore	ACC	NMI	ARI	Fscore	ACC	NMI	ARI	Fscore
Ours	73.91	71.60	57.89	66.94	82.62	72.31	65.80	73.09	67.58	56.93	46.71	57.22	53.33	40.48	28.82	40.21
(a) Effectiveness of Mask-informed Fusion Strategy																
wo-MFF	65.34	64.58	47.57	57.79	79.36	72.28	62.89	72.81	63.74	53.27	44.09	53.76	51.52	40.19	28.35	39.78
wo-MGF	70.76	69.16	53.69	64.29	80.97	71.28	64.45	72.36	66.45	55.88	47.72	56.32	51.98	39.40	27.05	39.26
(b) Effectiveness of Prior Knowledge-assisted Contrastive Learning																
wo-WCL	40.77	50.38	32.07	40.74	60.88	50.15	40.21	52.32	57.64	48.04	38.84	48.45	38.63	31.78	20.41	33.51
wo-Rec	74.29	71.72	57.65	66.79	75.57	69.26	58.35	68.27	67.97	57.10	47.11	57.33	52.96	41.37	24.62	41.59
w-CL	41.40	51.28	33.24	41.22	66.18	54.67	45.04	56.68	58.16	49.08	39.91	49.04	38.36	30.03	19.20	31.90
w-DCL	64.01	66.79	50.53	58.63	77.07	65.02	57.19	65.65	68.09	57.28	44.96	54.92	51.69	39.76	27.76	40.00

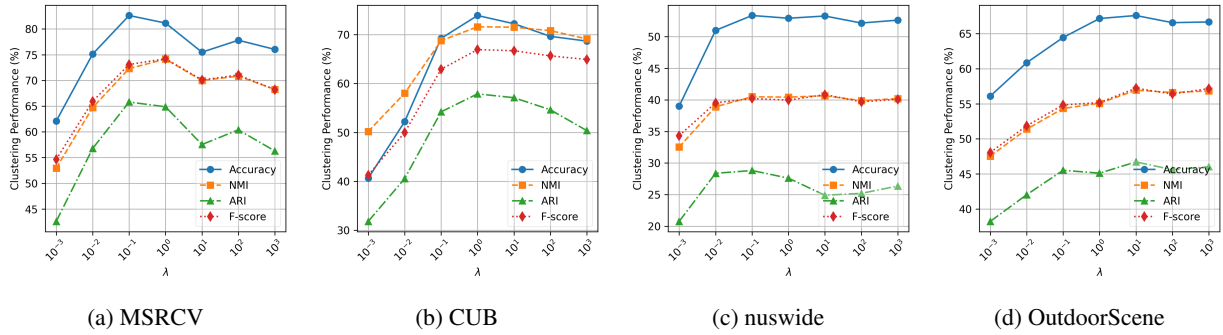


Figure 5. The parameter sensitivity of the proposed method on four multi-view datasets in terms of ACC, NMI, ARI, and Fscore, respectively.

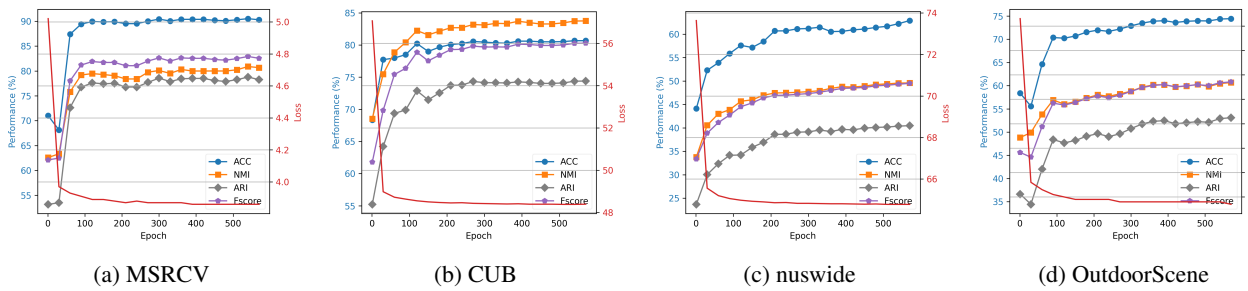


Figure 6. The convergence analysis of the proposed method on four benchmark multi-view datasets in terms of ACC, NMI, ARI, and Fscore, respectively.

A.2. Parameter sensitivity analysis

The parameter sensitivity analysis of the proposed method in terms of ACC, NMI, ARI, and Fscore on four benchmark multi-view datasets are given in Fig. 5.

A.3. Convergence analysis and visualization

The convergence analysis and visualization of the proposed method on four benchmark multi-view datasets are given in Figs. 6, 7, 8, 9, and 10.

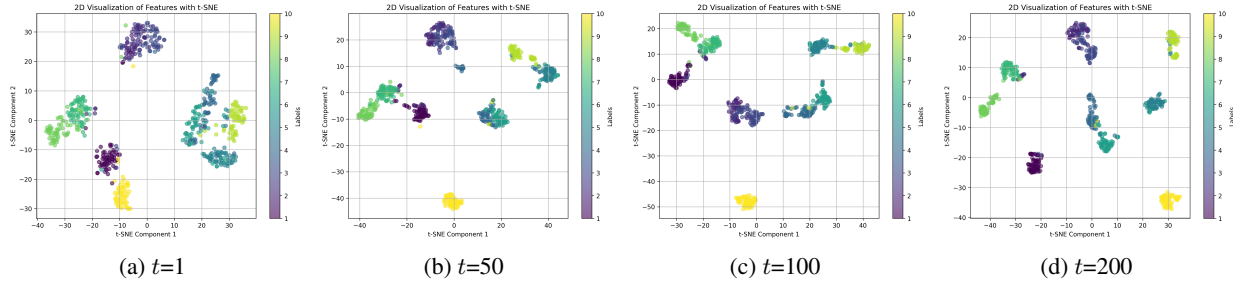


Figure 7. The visualization results of the proposed method under 1, 50, 100 and 200 epochs on CUB dataset.

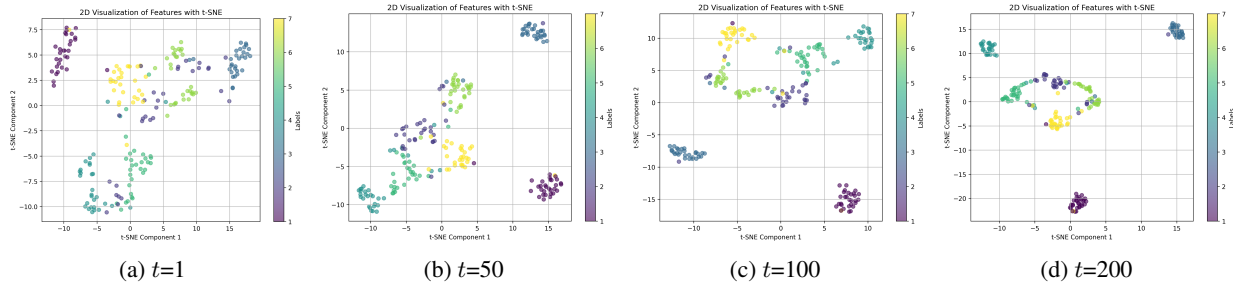


Figure 8. The visualization results of the proposed method under 1, 50, 100 and 200 epochs on MSRCV dataset.

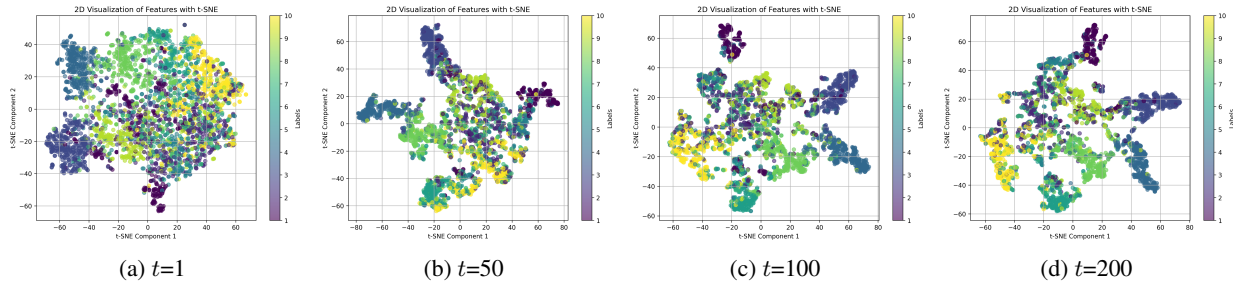


Figure 9. The visualization results of the proposed method under 1, 50, 100 and 200 epochs on nuswide dataset.

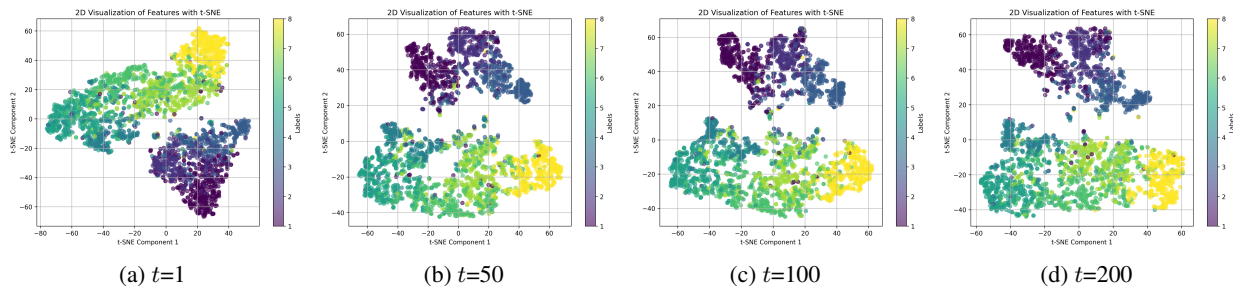


Figure 10. The visualization results of the proposed method under 1, 50, 100 and 200 epochs on OutdoorScene dataset.

B. Experimental Settings

B.1. Datasets

The details of four datasets are as follows:

MSRCV⁴: This dataset contains 210 images corresponding to seven different classes. Each image is characterized by three views: 256-dimensional LBP, 512-dimensional GIST, and 210-dimensional SIFT features.

CUB⁵: This dataset consists of 600 images of different bird species, each accompanied by text descriptions, spanning 10 categories. Each sample is represented by 4096-dimensional deep image features and 300-dimensional text features.

OutdoorScene (Hu et al., 2020): This dataset includes 2688 images of outdoor scenes captured from eight different scene groups. Each image is described using four views: 512-dimensional GIST features, 432-dimensional HOG features, 256-dimensional LBP features, and 48-dimensional Gabor features.

nuswide (Zhen et al., 2019): This dataset includes 9000 images along with corresponding tags from 10 categories. Each sample is represented by 4096-dimensional deep image features and 300-dimensional text features. We randomly selected 3000 samples in our experiments.

B.2. Implementation details

The detailed structures of the view-specific encoders and decoders are respectively D -196-128-64 and 64-128-196- D , where D denotes the input feature dimension. The PyTorch (Paszke et al., 2019) tool is utilized to implement the proposed method, in which the parameters are optimized with Adam optimizer (Kingma, 2014) with 0.001 initial learning rate. The proposed model is trained for 1500 epochs on all datasets, and the aggregated view-common feature representation is used to capture the cluster structures with the K-means. The features in all datasets are scaled into the range $[0, 1]$ in our experiments. the trade-off parameter λ in the proposed method is tuned in the range of $[10^{-3}, 10^{-2}, \dots, 10^2, 10^3]$. The number of neighbors in the formulated graphs is set to 15 for all datasets. All experiments are conducted on a single NVIDIA 2080Ti GPU with a Ubuntu 20.04 platform.

⁴<https://mldata.com/dataset/msrc-v1/>

⁵<https://www.vision.caltech.edu/visipedia/CUB-200.html>